Proceedings, MRS 1999 Fall Meeting, Boston, Mass., Nov. 29 - Dec. 3, 1999

PHOTOREFRACTIVE CONJUGATED POLYMER-LIQUID CRYSTAL COMPOSITES

M. R. WASIELEWSKI*, B. A. YOON*, M. FULLER*, G. P. WIEDERRECHT**, M. P. NIEMCZYK**, W. A. SVEC**
*Department of Chemistry, Northwestern University, Evanston, IL, 60208-3113
**Chemistry Division, Argonne National Laboratory, Argonne, IL, 60439-4831

ABSTRACT

A new mechanism for space-charge field formation in photorefractive liquid crystal composites containing poly(2,5-bis(2'-ethylhexyloxy)-1,4-phenylenevinylene) (BEH-PPV) and the electron acceptor N,N'-dioctyl-1,4:5,8-naphthalenediimide, NI, is observed. Using asymmetric energy transfer (beam coupling) measurements that are diagnostic for the photorefractive effect, the direction of beam coupling as a function of grating fringe spacing inverts at a spacing of 5.5 μm. We show that the inversion is due to a change in the dominant mechanism for space-charge field formation. At small fringe spacings, the space-charge field is formed by ion diffusion in which the photogenerated anion is the more mobile species. At larger fringe spacings, the polarity of the space charge field inverts due to dominance of a charge transport mechanism in which photogenerated holes are the most mobile species due to hole migration along the BEH-PPV chains coupled with interchain hole hopping. Control experiments are presented, which use composites that can access only one of the two charge transport mechanisms. The results show that charge migration over long distances leading to enhanced photorefractive effects can be obtained using conjugated polymers dissolved in liquid crystals.

INTRODUCTION

New organic materials that exhibit photorefractive effects are of wide interest for potential optical signal processing applications.[1-13] A particularly interesting class of materials for dynamic holography applications is photorefractive liquid crystals.[4-9,14-17] This is due to the efficiency of the nonlinear optical mechanism for photorefractivity in nematic liquid crystals coupled with the ease and cost effectiveness with which new samples can be prepared. The photorefractive effect itself is a light-induced change in the refractive index of a nonlinear optical material, resulting from the creation of an electric field induced by directional charge transport over macroscopic distances. If the material is electro-optic, the electric (or space-charge) field can then modulate the refractive index of the material.

In order to obtain a quantitative understanding of photorefractivity and fully exploit its optical signal processing possibilities, researchers usually induce the effect by means of a crossed laser beam technique.[18,19] When two beams of identical energy and spatial profile are overlapped in a sample, a sinusoidal interference pattern of light and dark regions is produced as illustrated in Figure 1. Charge separation occurs in the illuminated regions,

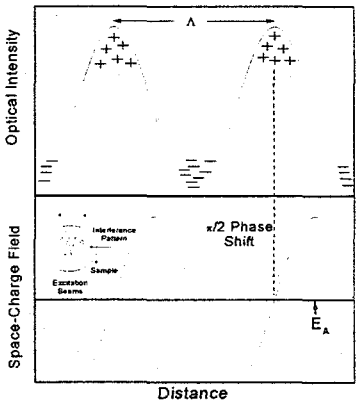

Figure 1. The phase relationship between the optical interference pattern and the space-charge field is illustrated. For liquid crystals, this example illustrates mobile anions migrating into the nulls of the interference pattern. The application of an applied electric field E_A is usually required to observe a phase shifted photorefractive grating.

DISCLAIMER

followed by charge migration. In liquid crystals, charge migration occurs through diffusion of ions until they ultimately reach the darker regions of the interference pattern. For a space charge field to form, the mobilities of the cation and anion must differ appreciably, or no space-charge field will form. This will permit one type of ion to remain preferentially in the illuminated region, while the more mobile ion diffuses into the dark region of the interference pattern. This produces a modulated space-charge field that can alter the refractive index of the material. The refractive index modulation, or grating, forms the basis for the optical signal processing applications of the photorefractive effect. Furthermore, the phase shift of the photorefractive grating relative to the optical interference pattern of approximately $\pi/2$, provides for asymmetric energy transfer from one excitation beam to the other. This leads to additional noise-free optical image amplification possibilities.

Liquid crystals owe their photorefractive sensitivity to high birefringence and ease of molecular reorientation in a space-charge field. The powerful nature of this effect can also be seen from improvements in the photorefractive polymer field, where many of the best materials use a low glass transition polymer to induce an orientational response of the poled, nonlinear optical molecules.[1] The orientational enhancement effect is frequently much greater than the normal electro-optic effect.[2,3] In both liquid crystals and polymers, the nonlinear index coefficient as given by the index of refraction change per unity optical intensity, is on the order of 0.01 to 0.1 cm^2/W.[2,3,20] These large nonlinear index coefficients are achieved in liquid crystals at very low applied electric fields of $<0.1 V/\mu m$, as opposed to applied fields of nearly $100 V/\mu m$ for many polymeric systems. [21] It should be noted that even higher values, up to 6 cm^2/W, have been reported for space-charge fields in liquid crystals generated without the application of an external field, which do not have the phase shift between the index grating and the optical interference pattern.[11]

Although nematic liquid crystals reorient easily in weak electric fields to produce an efficient electro-optic mechanism, inducing efficient charge transport in these materials is not as straightforward. Previous studies rely on photoinduced heterolytic cleavage of dye molecules or intermolecular electron transfer to create mobile anions and cations. These mobile charges obey the current density (J) equations given by: [22,23]

$$J = J^+ + J^- \tag{1}$$

$$J^{\pm} = q\mu^{\pm} n^{\pm}(x,t)\left(E_{SC}(x,t) - E_A\right)\mu\, qD^{\pm}\frac{\partial n^{\pm}[x,t]}{\partial x} \tag{2}$$

where $\mu^{\pm}$ is the mobility of the cations and anions, x is the grating wavevector axis, $n^{\pm}(x,t)$ is the ion density, $E_{SC}(x,t)$ is the magnitude of the space-charge field, E_A is the magnitude of the applied field, q is the unit charge, and $D^{\pm}$ is the diffusion constant of the cations and anions, respectively. The first term on the right hand side of equation 2 describes charge drift, and the second term describes ion diffusion. Previous studies of photorefractivity in liquid crystals indicate that ion diffusion is the charge transport mechanism that creates the space-charge field, a process that limits the efficiency and speed of the effect. The charge drift mechanism has not been a factor because of the short ionic drift length L_E, given by:

$$L_E = \frac{\mu^{\pm}\tau^{\pm}V}{d} \tag{3}$$

where $\tau^{\pm}$ is the carrier lifetime, V is applied potential, and d is the cell thickness.[22] Typically, $2\pi L_E << \Lambda$ in liquid crystals, while the drift mechanism can only contribute to a photorefractive grating if $2\pi L_E \geq \Lambda$.[22]

We now report on a photorefractive nematic liquid crystal composite containing the conjugated polymer poly(2,5-bis(2'-ethylhexyloxy)-1,4-phenylenevinylene), BEH-PPV that exhibits a novel fringe spacing dependent inversion of the polarity of the space-charge field due to competition between the ionic diffusion and charge drift transport mechanisms (Figure 2).

EXPERIMENT

A eutectic mixture of 35% (weight %) 4'-(*n*-octyloxy)-4-cyanobiphenyl, 8OCB and 65% 4'-(n-pentyl)-4-cyanobiphenyl, 5CB was doped with 10^{-5} M BEH-PPV (200 kD by GPC), as the electron donor.[24] The molecular weight of the BEH-PPV polymer implies that 500 repeat units of the monomer are present with an extended chain length of 0.35 μm. N,N'-dioctyl-1,4:5,8-naphthalenediimide, NI, $8x10^{-3}$ M, was added as the electron acceptor.[25] The free energy change for the photoinduced electron transfer reaction: ^{1*}(BEH-PPV) + NI → (BEH-PPV)$^{+}$ + NI^{-} is –1.0 eV.[26] Two other liquid crystal composites were also studied as controls. The first control composite contains the 5 unit phenylenevinylene oligomer, 5PV as the electron donor (4×10^{-5} M) along with 8 x 10^{-3} M NI acceptor.[27] The free energy change for the photoinduced electron transfer reaction: ^{1*}5PV + NI → 5PV^{+} + NI^{-} is –1.3 eV,[26] and is comparable to that for the BEH-PPV/NI pair. The second control composite contains 10^{-5} M BEH-PPV polymer with no NI present.

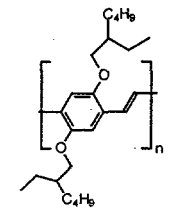

BEH-PPV

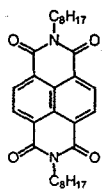

NI

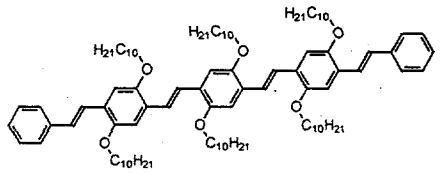

5PV

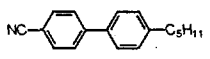

5CB

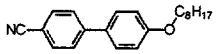

8OCB

Figure 2. The dopants and liquid crystal molecules are illustrated.

The liquid crystal composites are sandwiched between two indium tin oxide coated glass slides that are functionalized with n-octadecylsilyl groups to induce homeotropic alignment.[7] The cell thickness is 26 μm as determined by a Teflon spacer. The concentrations of BEH-PPV and 5PV used in these experiments provide equal absorbances of A = 0.02 at 514 nm. A 1.5 V potential is applied to the cell to induce both directional charge transport and the orientational photorefractive effect.[1] All of the composites exhibit a dark conductivity of approximately $4x10^{-11}$ S·cm^{-1}. The photo-conductivities of the composites using 514 nm, 1W·cm^{-2} irradiation are $1x10^{-10}$ S·cm^{-1} for both BEH-PPV/NI and 5PV/NI, and 3×10^{-11} S·cm^{-1} for the composite containing BEH-PPV alone.

Two coherent laser beams from an Ar^{+} laser with 1 mW total power at 514 nm and a beam diameter of 2.5 mm are overlapped in the sample to create an optical interference pattern.[6] For these composites, asymmetric energy transfer (beam coupling) from one of the crossed laser beams to the other is observed. This phenomenon is characteristic for the photorefractive effect, wherein the refractive index grating is phase shifted relative to the interference pattern.[19] Our experiments span the range of volume (Bragg) gratings at small Λ to thin (Raman-Nath) gratings

at large Λ. In the thin grating regime, other phenomena can also lead to the observation of asymmetric beam coupling, including thermal, photochromic, order-disorder, and phase change effects.[28] However, these possibilities are ruled out using diagnostic experiments that have been discussed previously.[7,12,15] For example, the direction of beam coupling reverses at all values of Λ, if the polarity of the applied static electric field is reversed. Additionally, the index grating is only observed for writing beams that are polarized with a component along x, consistent with an index change due to a modulated reorientation of the liquid crystal director and not to absorption effects.[15] As noted in other photorefractive studies in thin media, such as semiconductor quantum wells, the direction of beam coupling in both thin and thick grating regimes has the same dependence on the polarity of the space-charge field.[29]

RESULTS

Figures 3a and 3b show the kinetics of beam coupling for two different values of Λ in the BEH-PPV/NI composite and the control composite containing 5PV/NI. Comparing the data illustrated in Figure 3a with that in Figure 3b, the direction of beam coupling at smaller Λ is the same for both composites, while it is opposite for the two composites at larger Λ. Comparing Figures 4a and 4b for $\Lambda < 5.5$ μm, the direction of beam coupling in the BEH-PPV/NI composite is the same as that of the 5PV/NI control composite. A further observation is that beam coupling is observed in the BEH-PPV/NI composite at the high resolution $\Lambda = 1.5$ μm,[30] whereas the smallest Λ achieved with the 5PV/NI composite is 3 μm. These observations are consistent with a space-charge field created through an ion diffusion mechanism. Within this model, the magnitude of the space charge field in liquid crystals increases as the difference between the diffusion coefficients for the cation and anion increases.[12,15] NI^- has a larger diffusion coefficient than oxidized electron donors of comparable size, including $5PV^+$.[20,31] Since BEH-PPV$^+$ polymer cation has a much smaller diffusion coefficient than $5PV^+$, the space-charge fields derived from diffusion within both the BEH-PPV/NI and 5PV/NI composites should have the same polarity, and therefore, the same asymmetric energy exchange direction. The larger size and smaller diffusion coefficient of BEH-PPV$^+$ relative to that of $5PV^+$ results in a higher resolution grating attained with the BEH-PPV/NI composite

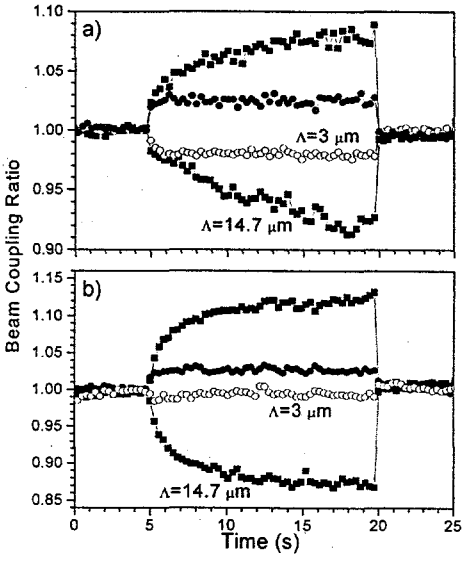

Figure 3. a) The kinetics of beam coupling in the BEH-PPV/NI liquid crystal composite is shown for Λ=14.7 μm (Φ and ϖ) and 3.0 μm (φ and ρ). b) The kinetics of beam coupling in the 5PV/NI liquid crystal composite is shown for Λ=14.7 μm (Φ and ϖ) and 3.0 μm (φ and ρ). The beam coupling ratio for beam 1 is I_{12}/I_1, where I_{12} is the intensity of beam 1, when both beam 1 and beam 2 are present in the sample, and I_1 is the intensity of beam 1 in the absence of beam 2. The corresponding beam coupling ratio for beam 2 is I_{21}/I_2, where I_{21} is the intensity of beam 2, when both beam 1 and beam 2 are present in the sample, and I_2 is the intensity of beam 2 in the absence of beam 1. Open symbols indicate the same beam, while solid symbols indicate the other beam. For each curve a photodiode monitors the intensity of one beam, while the other beam is incident on the sample at 5 s and blocked at 20 s.

because the difference in diffusion coefficients between BEH-PPV$^+$ and NI$^-$ is larger than that between 5PV$^+$ and NI$^-$.

The sign of the asymmetric beam coupling inverts for the BEH-PPV/NI composite at approximately $\Lambda = 5.5$ μm, while neither control composite shows this inversion. This suggests that the polarity of the space-charge field inverts at this point.[19] Comparing Figures 4a and 4b for $\Lambda > 5.5$ μm, the direction of beam coupling in the BEH-PPV/NI composite is the same as that with the control composite containing BEH-PPV alone. This indicates that the sign of the mobile charge carrier that contributes to space-charge field formation is the same for $\Lambda > 5.5$ μm in these two composites, and opposite to that for the control composite containing 5PV/NI. Therefore, since negative charges carried by diffusing NI$^-$ are the most mobile charges that contribute to a phase-shifted space-charge field in the BEH-PPV/NI composite for $\Lambda < 5.5$ μm, positive charges are the most mobile charges that contribute to a phase-shifted space-charge field at $\Lambda > 5.5$ μm.

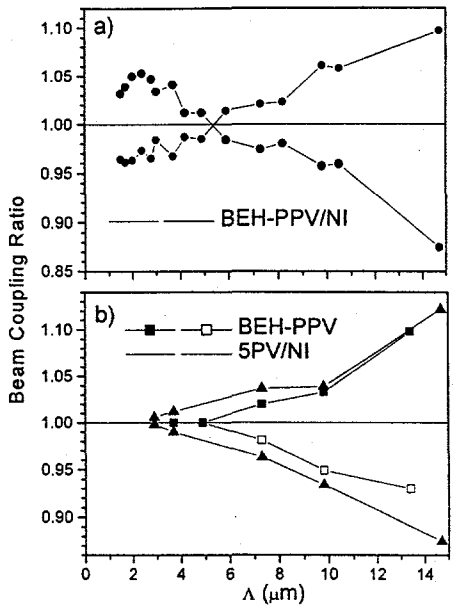

Figure 4. a) The magnitude and direction of beam coupling in the BEH-PPV/NI liquid crystal composite is shown. **b)** The beam coupling ratio vs Λ for the control composites containing only BEH-PPV or 5PV/NI is shown. Open symbols indicate the same beam for all three composites, while solid symbols indicate the other beam.

Since the high 200 kD molecular weight of BEH-PPV$^+$ precludes rapid ion diffusion, a charge migration mechanism other than diffusion is producing the space-charge field at larger values of Λ. Solutions of alkoxylated PPVs display very high intra-chain mobilities for both holes and electrons.[32,33] Fast hole transport along the BEH-PPV chain, coupled with hole hopping to other BEH-PPV chains can lead to long distance hole migration in the composite. This mechanism of charge transport can be considered a charge drift mechanism in the trap density limited regime. This means that the charge drift length, L_E, is larger in the BEH-PPV doped liquid crystals relative to the 5PV doped liquid crystals. In the context of equation 3, it is likely that $\tau^{\pm}$ and $\mu^{\pm}$ are significantly enhanced in the BEH-PPV polymer due to the delocalization of charge and fast intrachain hole mobilities. The increase in $\tau^{\pm}$ and $\mu^{\pm}$ through this mechanism is not possible for smaller cations and anions such as 5PV$^+$ and NI$^-$. Furthermore, the magnitude of the current density due to drift should be larger (eq. 2) in BEH-PPV doped composites because $n^{\pm}$ is proportional to the carrier lifetime.[22] Thus, L_E and $n^{\pm}$ are large enough in the BEH-PPV composite to observe charge drift as a contributor to space-charge field formation for the first time in liquid crystals.

The fringe spacing limit in which each charge transport mechanism dominates is consistent with our analysis. The contribution to the magnitude of the space-charge field derived from ion diffusion is inversely proportional to Λ.[12,15] However, the contribution to the space-charge field magnitude from charge drift, in the trap density limited model, is independent of Λ to a first approximation.[22] The space-charge field due to drift can contribute to the photorefractive grating as long as $2\pi L_E \geq \Lambda$ so that the space-charge field is phase-shifted from

the optical interference pattern. Therefore, in the BEH-PPV polymer/liquid crystal composites where L_E is enhanced, the charge drift mechanism should dominate space-charge field formation at the larger values of Λ explored in our experiments, but the ion diffusion mechanism should dominate at smaller Λ (Figure 2). Furthermore, the fact that the control composite containing only BEH-PPV does not show any beam coupling below 5.5 μm is consistent with the availability of only one charge transport mechanism, charge drift, because the absence of NI- precludes diffusional space charge fields at lower values of Λ. This discussion only applies to which charge transport mechanism will dominate space-charge field formation at a given fringe spacing. The magnitude of the space-charge field does not correlate with the beam coupling magnitude, because the orientational response of liquid crystals decreases at smaller fringe spacings for $\Lambda<2d$.[15]

We also performed polarized fluorescence spectroscopy on the BEH-PPV and 5PV doped liquid crystal cells in an effort to determine how the dopants were oriented. This is important because the alignment of the BEH-PPV or 5PV in the nematic liquid crystal host is expected to influence the magnitude of the space-charge field that contributes to the photorefractive effect. Charge migration must occur along the wavevector direction in order to achieve a modulation in the charge density. Furthermore, it has been shown that the orientation of the dopant relative to the liquid crystal alignment can be varied by altering the substituents on the dopant.[34]

The experimental geometry is illustrated in Figure 5. A polarizer is used to select either s (vertical in Figure 5) or p (horizontal in Figure 5) polarization of the excitation light. The liquid crystal cell is tilted by 45° relative to the incident excitation light. Since the cell is homeotropically aligned, the tilt angle is necessary for a component of the long axis of the liquid crystal molecules to be parallel to the horizontally polarized light. Thus, a measure of the fluorescence anisotropy is possible by measuring the fluorescence intensity for s and p polarized excitation. A Photon Technologies International fluorimeter is used for data collection.

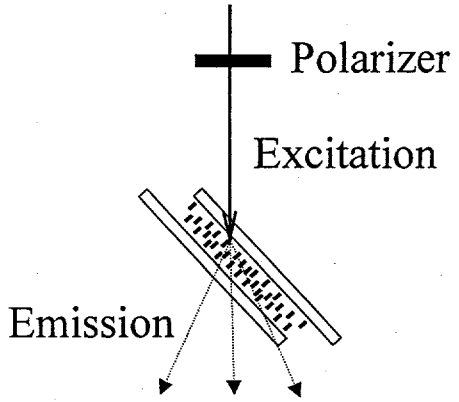

Figure 5. The experimental geometry for fluorescence anisotropy measurements is shown.

The data for the fluorescence anisotropy of 5PV and BEH-PPV in the liquid crystal cells are shown in Figures 6 and 7, respectively. The data shows that the 5PV has greater fluorescence intensity for p polarized excitation, indicating that it lies oriented with the long axis parallel to the liquid crystal director. On the other hand, the BEH-PPV polymer shows little fluorescence anisotropy, indicating that there is no preferred alignment of the polymer chain in the liquid crystal. New substituents will have to be designed in order to optimize directional charge transport with these polymer/liquid crystal composites.

It is well known that the phase behavior of stiff-chain polymers can be significantly modified by adding flexible appendages to the stiff chains[35]. In favorable cases the resultant polymers exhibit liquid crystalline phases[36,37]. A similar strategy may be employed in liquid crystalline composites using soluble PPV derivatives, Figure 8. The side chains on the polymers shown in Figure 8 are designed to provide a means of orienting the conductive PPV backbone within a nematic liquid crystal in an orientation that is roughly parallel to the direction of the grating wavevector and perpendicular to the director of the liquid crystal [38]. This is the ideal orientation for promoting the formation of larger space charge fields in the correct direction to interact strongly with the electric fields of the laser beams to maximize the photorefractive

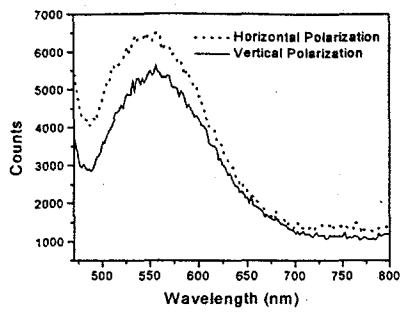

Figure 6. The fluorescence anisotropy of the BEH-PPV doped composites is illustrated.

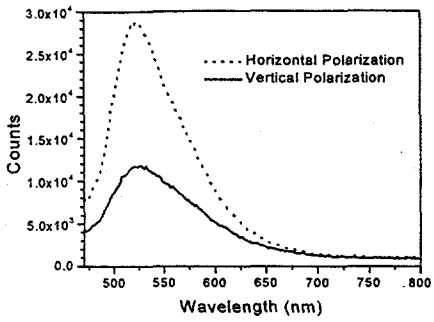

Figure 7. The fluorescence anisotropy of the BEH-PPV doped composites is illustrated.

response. The syntheses of these polymers are in progress. The polymer with the side chains that have a structure similar to 5CB is particularly interesting from the standpoint of controlling the orientation of the conjugated path of the polymer relative to the director of the nematic liquid crystal. In this particular case the dominance of the drift mechanism for charge transport at small values of Λ combined with increased charge migration along the wavevector direction should yield increased diffraction efficiencies and beam coupling ratios, while maintaining these characteristics in the Bragg grating regime.

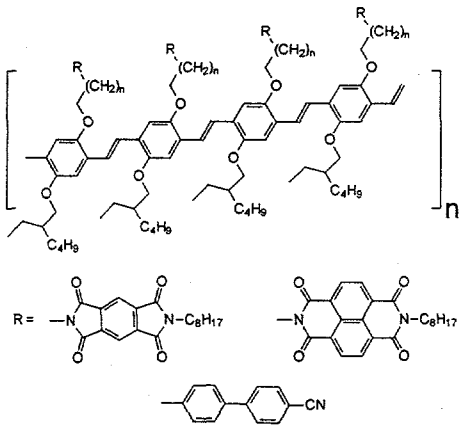

Figure 8. Conjugated polymers for increased response time in photorefractive liquid crystal composites.

CONCLUSIONS

We have shown that the BEH-PPV conjugated polymer provides a mechanism to enhance the photorefractive effect in each fringe spacing limit. In the ion diffusion limit, the much lower mobility of BEH-PPV$^+$ relative to that of NI$^-$ decreases the fringe spacing in which photorefractive beam coupling can be observed. Furthermore, the use of BEH-PPV enhances the charge drift length so that a new space-charge field generation mechanism in liquid crystals becomes possible. Fluorescence anisotropy measurements indicate that the BEH-PPV does not significantly orient relative to the direction of the liquid crystal director within the sandwich cell used to carry out the photorefractivity measurements. Polymers that utilize side groups that are similar to the nematic liquid crystals themselves may provide a means of actively controlling the orientation of the conjugated polymer relative to the director of the liquid crystal. Since the director of the liquid crystal can be easily aligned perpendicular to the plane of the ITO coated glass surface within the cell, this functionalization strategy may provide a means of self-assembling the orientation that is most desirable for enhancing the photorefractive properties of these composites. The versatility of conjugated polymers in enhancing the photorefractive effect in liquid crystal composites may lead to the development of new optical devices that use photorefractivity for information processing and storage.

ACKNOWLEDGMENTS

We gratefully acknowledge support from the Office of Naval Research under grant No. N00014-99-1-0411 (MRW) and the Technology Research Division, Office of Advanced Scientific Computing Research, U.S. Department of Energy, under contract W-31-109-ENG-38 (GPW).

REFERENCES

1 W. E. Moerner, S. M. Silence, F. Hache, and G. C. Bjorklund, *J. Opt. Soc. Am. B* **11,** 320-30 (1994).

2 K. Meerholz, B. L. Volodin, Sandalphon, B. Kippelen, and N. Peyghambarian, *Nature* **371,** 497-500 (1994).

3 A. Grunnet-Jepsen, C. L. Thompson, R. J. Twieg, and W. E. Moerner, *Appl. Phys. Lett.* **70,** 1515-1517 (1997).

4 E. V. Rudenko and A. V. Sukhov, *JETP Lett.* **59,** 142-46 (1994).

5 I. C. Khoo, H. Li, and Y. Liang, *Opt. Lett.* **19,** 1723-25 (1994).

6 G. P. Wiederrecht, B. A. Yoon, and M. R. Wasielewski, *Science* **270,** 1794-97 (1995).

7 G. P. Wiederrecht and M. R. Wasielewski, *J. Am. Chem. Soc.* **120,** 3231-3236 (1998).

8 A. Golemme, B. L. Volodin, B. Kippelen, and N. Peyghambarian, *Opt. Lett.* **22,** 1226-28 (1997).

9 H. Ono, I. Saito, and N. Kawatsuki, *Appl. Phys. Lett.* **72,** 1942-44 (1998).

10 P. M. Lundquist, R. Wortmann, C. Geletneky, R. J. Twieg, M. Jurich, V. Y. Lee, C. R. Moylan, and D. M. Burland, *Science* **274,** 1182-85 (1996).

11 I. C. Khoo, S. Slussarenko, B. D. Guenther, M.-Y. Shih, P. Chen, and W. V. Wood, *Opt. Lett.* **23,** 253-255 (1998).

12 E. V. Rudenko and A. V. Sukhov, *JETP* **78,** 875-882 (1994).

13 Q. Wang, L. M. Wang, and L. P. Yu, *J. Am. Chem. Soc.* **120,** 12860-12868 (1998).

14 H. Ono, *Opt. Lett.* **22,** 1144-46 (1997).

15 I. C. Khoo, *IEEE J. Quant. Elec.* **32,** 525-534 (1996).

16 G. Cipparrone, A. Mazzulla, and F. Simoni, *Opt. Lett.* **23,** 1505 (1998).

17 N. V. Tabiryan and C. Umeton, *J. Opt. Soc. Am. B* **15,** 1912-17 (1998).

18 C. R. Giuliano, *Physics Today* **April,** 27-35 (1981).

19 P. Gunter and J. P. Huignard, *Photorefractive Materials and Their Applications 1: Fundamental Phenomena* (Springer-Verlag, Berlin, 1988).

20 G. P. Wiederrecht, B. A. Yoon, and M. R. Wasielewski, *Adv. Mat.* **8,** 535-39 (1996).

21 W. E. Moerner, A. Grunnet-Jepsen, and C. L. Thompson, *Annu. Rev. Mater. Sci.* **27,** 585-623 (1997).

22 P. Gunter, *Phys. Rep.* **93,** 199-299 (1982).

23 B. Maximus, E. D. Ley, A. D. Meyere, and H. Pauwels, *Ferroelectrics* **121,** 103-112 (1991).

24 B. Wang and M. R. Wasielewski, *J. Am. Chem. Soc.* **119,** 12-21 (1997).

25 S. R. Greenfield, W. A. Svec, D. Gosztola, and M. R. Wasielewski, *J. Am. Chem. Soc.* **118,** 6767-6777 (1996).

26 The oxidation potentials, E_{OX} of BEH-PPV and 5PV are both 0.9 V vs SCE, respectively, while their lowest excited state energies, E_S are 2.4 eV and 2.7 eV, respectively. The reduction potential, E_{RED} of NI is –0.5 V vs SCE. ΔG for photoinduced electron transfer is estimated as $E_{OX} - E_{RED} - E_S$.

27 5PV was prepared by Wittig reaction of two moles of benzyltriphenylphosphonium bromide with the terminal dialdehyde of the corresponding three unit phenylenevinylene oligomer reported earlier.[24]

28 I. C. Khoo, *Opt. Lett.* **20,** 2137-39 (1995).

29 Q. Wang, R. M. Brubaker, D. D. Nolte, and M. R. Melloch, *J. Opt. Soc. Am. B* **9,** 1626-41 (1992).

30 BraggRegime, .

31 G. P. Wiederrecht, B. A. Yoon, and M. R. Wasielewski, *Synth. Met.* **84,** 901-2 (1997).

32 R. J. O. M. Hoofman, M. P. D. Haas, L. D. A. Siebbeles, and J. M. Warman, *Nature* **392,** 54-56 (1998).

33 W. B. Davis, W. A. Svec, M. A. Ratner, and M. R. Wasielewski, *Nature* **396,** 60-63 (1998).

34 H. Levanon, *Chem. Phys. Lett.* **90,** 465-71 (1982).

35 M. Ballauff, *Angew. Chem. Int. Ed. Engl.* **28,** 253-267 (1989).

36 G. Wegner, *Thin Solid Films* **216,** 105-116 (1992).

37 U. Lauter, W. H. Meyer, and G. Wegner, *Macromolecules* **30,** 2092-2101 (1997).

38 S. Michaeli, M. Hugerat, H. Levanon, M. Bernitz, A. Natt, and R. Neumann, *J. Am. Chem. Soc.* **114,** 3612-18 (1992).